


Efficacy of Ethyl Acetate Fraction of *Cordyceps militaris* for Cancer-Related Fatigue in Blood Biochemical and ¹H-Nuclear Magnetic Resonance Metabolomic Analyses

Integrative Cancer Therapies
Volume 19: 1–12
© The Author(s) 2020
Article reuse guidelines:
sagepub.com/journals-permissions
DOI: 10.1177/1534735420932635
journals.sagepub.com/home/ict


Junsang Oh, PhD^{1,2,*}, Eunhyun Choi, PhD^{1,2,*} , Jayoung Kim, MD, PhD^{2,3}, Heesu Kim, MD^{2,4}, Sangheun Lee, MD, PhD^{2,5}, and Gi-Ho Sung, PhD^{1,2,6}

Abstract

This study investigated the adjuvant effects for anticancer and antifatigue of the combination of *Cordyceps militaris* extract with sorafenib. The 5 extracts of *C. militaris* were obtained through hexane, chloroform, ethyl acetate, butanol, and water and were evaluated for anticancer growth activity. Among these extracts, ethyl acetate extract of *C. militaris* showed the best tumor growth inhibitory activity and the adjuvant effects in combination with sorafenib. As a result of biochemical analysis with serum, the combination of ethyl acetate extract of *C. militaris* with sorafenib showed the adjuvant effects both improving hepatic function and relieving cancer-related fatigue. In addition, ¹H-nuclear magnetic resonance–based metabolic profiling in liver tissues showed that the change of metabolism by ethyl acetate extract of *C. militaris* with sorafenib was related with serum fatigue biomarkers. Therefore, the combination strategy such as ethyl acetate extraction of *C. militaris* with sorafenib constitutes a promising therapeutic strategy in hepatocellular carcinoma, via the inhibition of cancer growth, the enhancement of liver function, as well as the alleviation of cancer-related fatigue.

Keywords

cancer-related fatigue, hepatocellular carcinoma, *Cordyceps militaris*, ethyl acetate fraction, xenograft mouse model, ¹H-NMR metabolic profiling

Submitted October 29, 2019; revised April 17, 2020; accepted May 17, 2020

Introduction

Liver cancer is the second most common cause of cancer-related death worldwide, and hepatocellular carcinoma (HCC) is the most common type of liver cancer.¹ Sorafenib (Nexavar), an orally bioavailable multikinase inhibitor, is well known to block tumor angiogenesis and tumor cell proliferation and approved by the Food and Drug Administration for the treatments of patients with advanced HCC. Although some benefits were observed in the initial clinical studies, the efficacy of sorafenib against HCC was mild or mild-to-moderate due to drug resistance, drug insensitivity, and various adverse events.^{2,3} The common adverse effects of sorafenib in HCC include loss of appetite, weight loss, rash development, diarrhea, abdominal pain, swelling, fatigue, alopecia, and high blood pressure.⁴ To obtain the synergistic effects and alleviate the side effects of sorafenib, a number of studies have investigated the combination treatment

¹Translational Research Division, Biomedical Institute of Mycological Resource, International St. Mary's Hospital, Incheon, Republic of Korea

²College of Medicine, Catholic Kwandong University, Gangneung, Republic of Korea

³Department of Laboratory Medicine, International St. Mary's Hospital, Incheon, Republic of Korea

⁴Department of Dermatology, International St. Mary's Hospital, Incheon, Republic of Korea

⁵Department of Internal Medicine, International St. Mary's Hospital, Incheon, Republic of Korea

⁶Department of Microbiology, College of Medicine, Catholic Kwandong University, Gangneung, Republic of Korea

*Junsang Oh and Eunhyun Choi contributed equally to this work.

Corresponding Author:

Gi-Ho Sung, Translational Research Division, Biomedical Institute of Mycological Resource, International St. Mary's Hospital and Department of Microbiology, College of Medicine, Catholic Kwandong University, Gangneung, Republic of Korea.
Email: sung97330@gmail.com



with other therapeutic agents, including kinase inhibitor regorafenib,⁵ histone deacetylase inhibitor panobinostat,⁶ nonsteroidal anti-inflammatory drug celecoxib,⁷ and natural products such as *Sophora flavescens* and *Scutellaria baicalensis* Georgi.^{8,9} However, contrary to expectations, the results of the chemoreagent combination therapies showed neither improved survival rates nor reduced adverse effects.¹⁰

Fatigue is one of the representative side effects experienced by cancer patients, and a number of studies have been addressing these adverse effects.¹¹⁻¹³ Cancer-related fatigue is defined as a distressing, persistent subjective mental tiredness, or exhaustion accompanying cancer treatment.¹⁴ Fatigue is influenced by the level of some amino acids in plasma and changes the plasma metabolic profiles.¹⁵ Lactate dehydrogenase (LDH), creatine kinase, glucose (GLU), and glutathione peroxidase are used as fatigue biomarkers.^{16,17} Inducible fatigue is associated with increased LDH and creatine kinase levels, accompanied by decreased GLU and glutathione peroxidase levels in serum.¹⁸ The blood LDH level reflects the degree of muscle damage and the regulation of glycolysis and lactate metabolism.¹⁹ In addition, the GLU levels have been evaluated to monitor energy consumption and the accumulation of unnecessary metabolites in serum.²⁰ The antifatigue agent salidroside works by delaying lactate accumulation, suppressing glycolysis, or enhancing the rate of blood lactate removal,²¹ and the oral administration of Hwanggi (*Astragalus Radix*), a traditional medicinal plant, decreases lactate levels and increases blood GLU levels in rats, which is related to the typical antifatigue effect.²²

Cordyceps militaris (Ascomycota; Hypocreales; Cordycipitaceae), an entomopathogenic fungus, is one of most important medicinal mushrooms.²³⁻²⁵ The chemical constituents of *C. militaris* include cordycepin, adenosine-like nucleoside, cordycepic acid (mannitol), ergosterol, amino acids, and polysaccharides.^{26,27} Either ethanol or water extracts of *C. militaris* showed anticancer, antifatigue, and antihypoxic activities.²⁷⁻³²

Metabolomics is an important scientific tool for delineating biological systems or phenomena through metabolite profiling within cells, biofluids, tissues, or organisms, and is based on nuclear magnetic resonance (NMR) spectroscopy and mass spectrometry with multivariate statistical analysis.³³ Using the ¹H-NMR coupled with multivariate statistical analysis, Song and colleagues showed that Hwanggi had anti-fatigue effects as a result of the metabolic pathway changes including glycometabolism, lipid metabolism, and energy metabolism.²⁹

Currently, studies of the antifatigue or anticancer effects of *C. militaris* have been published,^{34,35} but the direct relationship to cancer-related fatigue of *C. militaris* has not been reported yet. In this study, we investigated the HCC growth inhibitory activity and the improvement in cancer-related fatigue by the extract of *C. militaris* as a single administration and in combination with sorafenib. In addition, we demonstrated the mechanism of improving

cancer-related fatigue using NMR-based metabolomic analysis in liver tissues and biochemical analysis in blood serum from xenograft mouse models.

Materials and Methods

Chemical Reagents

Ethanol, methanol, *n*-hexane, chloroform, ethyl acetate, *n*-butanol, and water were purchased from Honeywell Burdick & Jackson. RPMI-1640 medium and fetal bovine serum were obtained from GIBCO Life Technologies. The analytical reagents of serum levels of alkaline phosphatase (ALP), alanine aminotransferase (ALT), aspartate aminotransferase (AST), bilirubin (BIL), cortisol, γ -glutamyl transpeptidase (γ -GTP), GLU, and LDH were purchased from Beckman Coulter. Deuterium oxide (D₂O, 99.9% D), NaH₂PO₄, K₂HPO₄, 3-(4,5-dimethylthiazol-2-yl)-2,5-diphenyltetrazolium bromide, and antibiotics (eg, penicillin and streptomycin) were obtained from Sigma-Aldrich, and sodium 3-(trimethylsilyl)-propionic-2,2,3,3-d₄ acid sodium salt (TSP) was obtained from Cambridge Isotope Laboratories.

Extraction and Fractionation of *Cordyceps militaris*

The fruiting bodies of *C. militaris* were kindly supplied by Cordyceps Research Institute at Mushtech (Hoengseong, Gangwondo, Korea). The fruiting bodies were produced by inoculating fungal liquid spawn on brown rice medium. The fruiting bodies including brown rice medium were crushed in a blender and the crude powder was extracted with 95% ethanol at 80 °C for 3 hours. The extracts were evaporated at 60 °C under pressure and resuspended in distilled water. The aqueous layer was mixed with *n*-hexane, shaken, and then the *n*-hexane layer was separated. Chloroform, ethyl acetate, butanol, and aqueous fractions were processed following the same method (Figure 1). Finally, each solvent fraction was evaporated and freeze-dried under pressure.

Huh-7 Cell Culture and Cytotoxicity Assay

Huh-7 cell line (Korean Cell Line Bank, Seoul, Korea) was cultured in complete RPMI-1640 medium supplemented with 10% fetal bovine serum, 100 IU/mL penicillin, and 100 μ g/mL streptomycin. The cells were incubated at 37 °C in a humidified atmosphere containing 5% CO₂. Cytotoxicity of *C. militaris* extracts on Huh-7 cells was evaluated by MTT (3-(4,5-dimethylthiazol-2-yl)-2,5-diphenyltetrazolium bromide) assays. Briefly, cells were plated in 96-well plates at 1×10^4 cells/well. After 24-hour incubation, the cells were treated with various concentrations of the *Cordyceps militaris* ethyl acetate extract fraction (CMEAF) for 24 hours. At the end of the incubation, 50 μ L of the MTT solution (3 mg/mL in phosphate-buffered saline) was added to each well. After 2-hour incubation, the medium containing

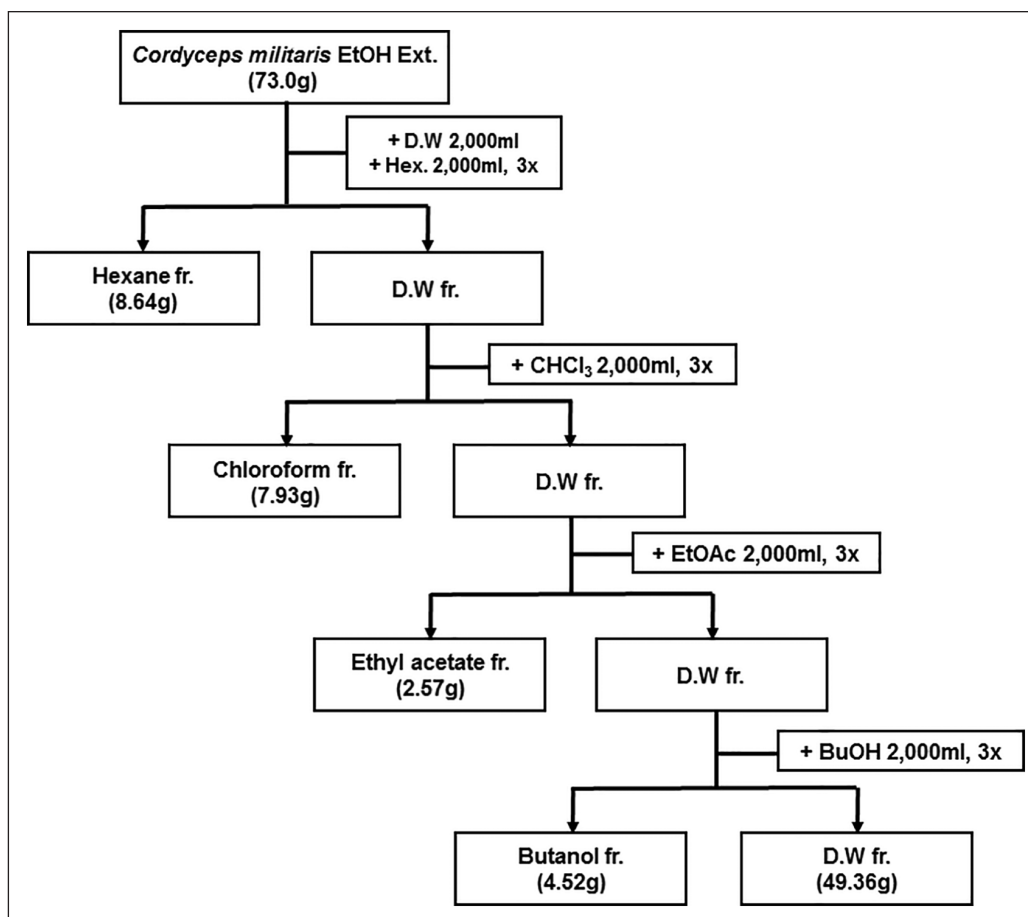


Figure 1. Fractionation scheme of *Cordyceps militaris*. Protocol for the best series of solvent fractionation of ethanol *Cordyceps militaris* extract. Finally, 8.64 g of *n*-hexane extract fraction, 7.93 g of chloroform extract fraction, 2.57 g of ethyl acetate extract fraction, 4.52 g of *n*-butanol extract fraction, and 49.36 g of water extract fraction were collected.

MTT solution was replaced with isopropanol for extraction of dye. After incubation for 30 minutes, absorbance was measured on VERSAmax microplate reader (Molecular Devices) at 570 nm.

Xenograft Mouse Model

Five-week-old female BALB/c-nu Slc mice were purchased from Orent Bio Inc. Mice were housed in a temperature-controlled animal facility with a 12-hour light/dark cycle (with light intensity of 150-300 Lux) and a relative humidity of $55 \pm 15\%$ at $23 \pm 3^\circ\text{C}$. All the mice consumed a commercial diet (Teklad certified irradiated global 18% protein rodent diet; 2918C, ENVIGO) and water ad libitum. Tumors were generated by subcutaneous injection of 5×10^6 Huh7 cells/0.1 mL over the flank of the mouse. The body weight and tumor size were measured twice a week. The tumor volume was calculated using the formula $\text{volume} = (\text{width}^2 \times \text{length})/2$ (mm^3).⁹ When tumor volume reached 75 to 100 mm^3 , mice were randomly divided into 4 groups ($n = 4/$

group): (1) control group, (2) CMEAF treatment group (50 mg/kg of body weight), (3) sorafenib treatment group (30 mg/kg), and (4) CMEAF (50 mg/kg) with sorafenib (30 mg/kg) treatment group. The mice were orally administered with *C. militaris* fraction or sorafenib once daily for 19 days. On day 19, mice were sacrificed, serum and liver tissue obtained from the mice at necropsy were stored at -75°C until further study. All animal experiments were conducted in accordance with the National Guidelines for Experimental Animal Care Policies. The study protocol was reviewed and approved by the Institutional Animal Care and Use committee of the Gyeonggi BioCenter (Protocol No. GGBC, 2017-02-0001).

Serum Biochemical Analysis

Blood chemistry measurements were performed using AU5800 clinical chemistry analyzer (Beckman Coulter). Mouse serum was sampled for chemistry parameters (LDH, GLU, AST, ALT, ALP, BIL, and γGTP). Serum

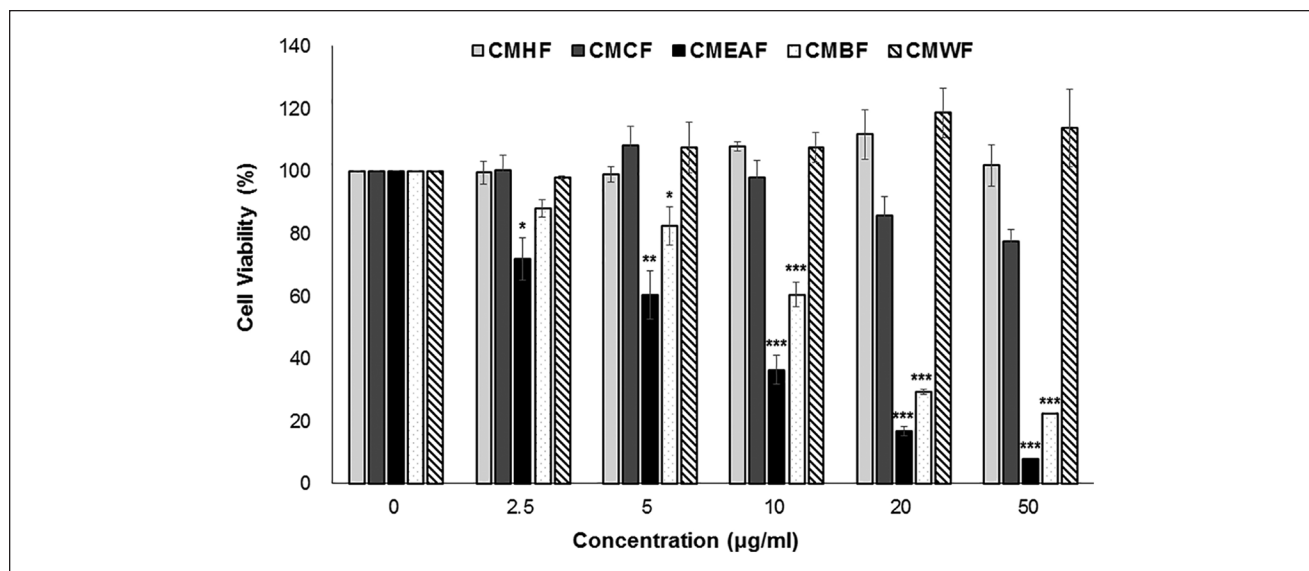


Figure 2. In vitro screen cell cytotoxicity of Huh-7 cells. Cells were treated with various concentrations of different fraction of *Cordyceps militaris* for 24 hours and cell viability was determined by the MTT assay. Results are expressed as percentages of proliferation compared with the untreated control (mean \pm standard deviation). * $P < .05$; ** $P < .01$; *** $P < .001$ compared with control. Abbreviations: CMHF, *n*-hexane extract fraction; CMCF, chloroform extract fraction; CMEAF, ethyl acetate extract fraction; CMBF, *n*-butanol extract fraction; CMWF, water extract fraction.

cortisol was measured by UniCel DxI 800 system (Beckman Coulter).

¹H-NMR Analysis of Liver Tissues

For metabolomic extraction of liver tissue samples, 0.2 g of frozen liver tissues were weighed and homogenized in the mixture solution of 800 μ L of methanol and 170 μ L of DW using TissueLyser LT (QIAGEN) for 1 minute. After disruption, samples were mixed with 800 μ L of chloroform and 400 μ L of DW and then kept on ice for 20 minutes. The mixture was centrifuged at 1000 *g* for 15 minutes at 4 $^{\circ}$ C. The 600 μ L of supernatant was transferred into a vial and dried in TOMY Micro Vac MV-100 Vacuum Centrifugal Evaporator (TOMY) at room temperature. After drying, samples were resuspended in 600 μ L of phosphate buffer (pH 7.0-7.4) in D₂O containing 0.01% TSP. This mixture was vortexed and then centrifuged at 12 000 rpm for 10 minutes and collected into a 5 mm NMR tubes (Norell). ¹H-NMR spectra were acquired on a Bruker Advance Spectrometer (Bruker BioSpin GmbH), operating at a 600.13-MHz frequency, using the standard CPMG spin echo pulse sequence with water presaturation to suppress the water signal and a total spin-spin relaxation delay of 2 seconds was used. In total, 128 transients were recorded into 32K data points over a spectral width of 20 ppm (F2) and 40 Hz (F1), resulting in an acquisition time per scan of 1.36 seconds.

Data Preprocessing and Statistical Analysis

All spectra were phased manually, and baseline corrected on Chenomx software (ver 8.2, Edmonton, Canada). Spectral calibration was performed using TSP δ 0.00 for all tissues. The spectral region δ 0.6 to 10.00 was segmented into bins of 0.04 ppm and the regions of δ 4.60 to 4.80 were discarded prior to analysis to attenuate the residual water resonance. Characteristic peaks of the metabolites were identified based on comparisons with the Chenomx software suite database and Human Metabolome Database (<http://www.hmdb.ca/>). Multivariate statistical analysis was performed with only 40 metabolites qualified from Chenomx software (version 8.2).

Each spectral intensity dataset was normalized to the total sum of the spectral regions. The significant differences in metabolite levels were detected by one-way analysis of variance using the SPSS statistics software (version 22.0, SPSS Inc) followed by the Duncan's significant-difference test. The level of statistical significance was set at $P < .05$. Principal component analysis (PCA) was performed using SIMCA software (version 14.0, Umetrics). In addition, orthogonal projection to the latent structure with discriminant analysis (OPLS-DA) was performed with UV scaling. Qualities of the OPLS-DA models were evaluated with R^2X for the explained variation and Q^2 for the model predictabilities. We also calculated the variable importance in the projection (VIP) value and $p(\text{corr})$ to further evaluate the results of OPLS-DA

analyses. While the $p(\text{corr})$ value is stable compared with the VIP value when selecting iterative variables and can be compared between models. Therefore, it is often difficult to determine the optimal model based on the value of the VIP alone and $p(\text{corr})$ value is used together to maximize the statistical power.

Results

In Vitro Anti-Proliferation Effect on Huh-7 of Extract Fractions of *Cordyceps militaris*

The anticancer effect of *C. militaris* has been intensively studied for various cancer cell lines including HCC.²⁷ We performed in vitro screening of the growth inhibition of Huh-7 cells with 5 extract fractions of *C. militaris*, *n*-hexane (CMHF), chloroform (CMCF), ethyl acetate (CMEAF), *n*-butanol (CMBF), and water (CMWF; Figure 1). Among these extract fractions, CMEAF showed significantly more inhibition of the growth of Huh-7 than other fractions in a dose-dependent manner (Figure 2); therefore, we selected CMEAF for the in vivo xenograft experiment and investigated anticancer and anti-fatigue effects by the treatment with this fraction either alone or in combination with sorafenib.

In Vivo Efficacy of CMEAF Administration Either Alone or in Combination With Sorafenib

To confirm the adjuvant effect of anticancer, the CMEAF (50 mg/kg) and sorafenib (30 mg/kg) were orally administered once a day for 19 days. Compared with control group, CMEAF, sorafenib, and the combined treatment groups showed a decrease in tumor volume approximately 39%, 52%, and 56%, respectively (Figure 3A), and tumor weight (Figure 3B) without inducing weight loss (Figure 3C). However, there was no the statistically significant between in each treatment group of CMEAF and sorafenib and the combined treatment group ($P > .05$).

Improving Hepatic Function and Anti-Fatigue Effects of CMEAF

Because *C. militaris* has an influence on liver function and relieving fatigue^{31,36} and hepatic function is tightly linked to cancer-related fatigue, we hypothesized that CMEAF might be associated with improving hepatic function and fatigue against either cancer or sorafenib. The increase in AST and ALT levels in blood serum indicate liver damage or chronic liver disease,^{37,38} whereas the increase in ALP is related to improving hepatic function.³⁹ As shown in Figure 4A, the levels of AST and ALT showed no significant difference, whereas ALP activity showed significant increases in both

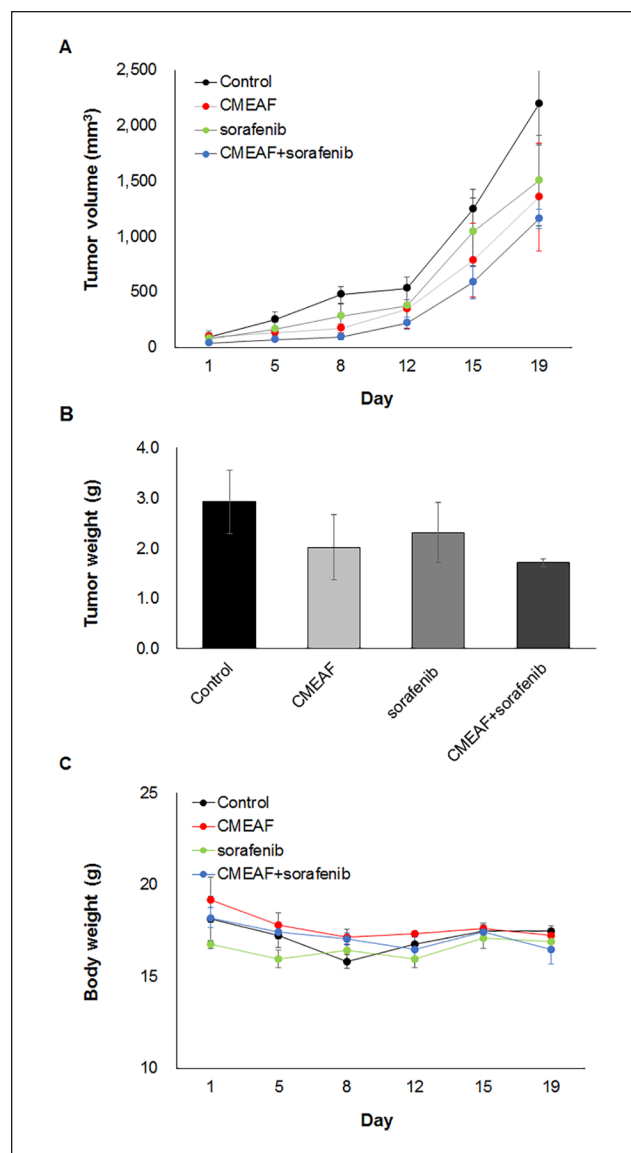


Figure 3. Tumor volume, tumor weight, and body weight after treatment in BALB/c Slc-nu/nu mice with Huh-7 xenograft models. The control, *Cordyceps militaris* ethyl acetate extract fraction (CMEAF; 50 mg/kg), sorafenib (30 mg/kg), or CMEAF with sorafenib ($n = 4$ per group) daily and body weights were recorded for a period of 19 days. (A) Tumor volume was recorded using caliper measurements as described in Materials and Methods. (B) Tumor weights were obtained at the end of the study. (C) Body weights of the treated mice were compared with animals that received vehicle control. Data are expressed as means \pm standard error of the mean ($n = 4$ per group). No statistically significant difference, $P > .05$.

CMEAF and CMEAF with sorafenib groups. In addition, the decrease level of BIL and the increase level of γ GTP in CMEAF treatment group indicated liver function is improved.

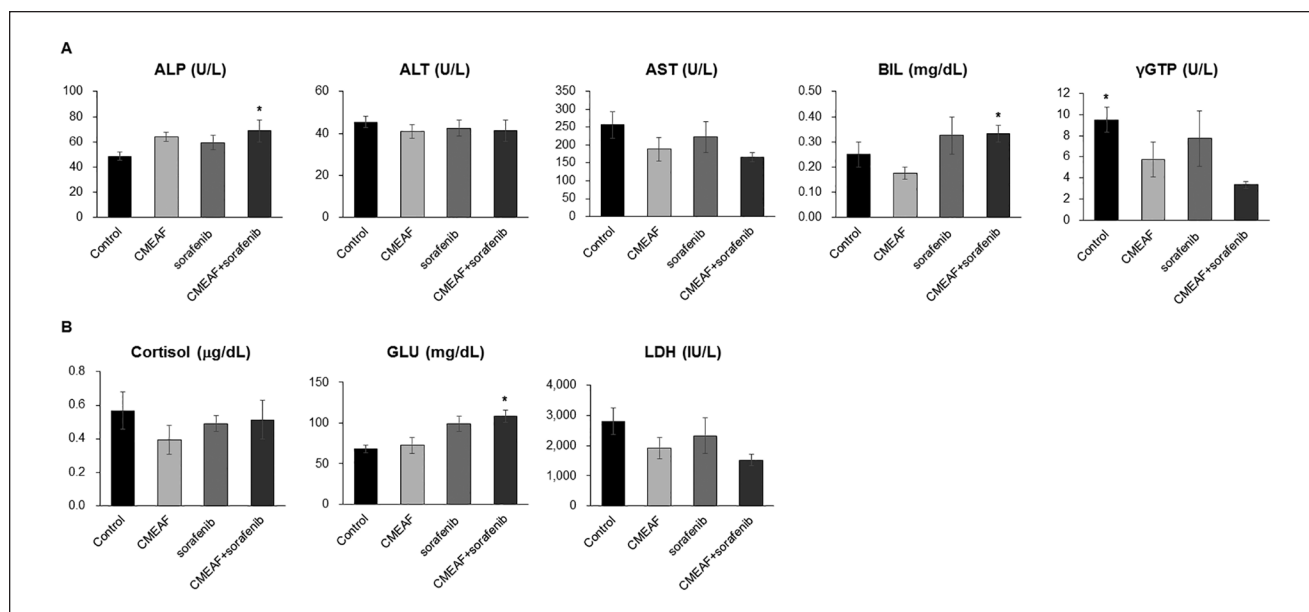


Figure 4. Relative quantification of plasma biomarkers by biochemical assay. (A) Changes in relative quantification of plasma in hepatotoxicity and liver function with ALP, ALT, AST, BIL, and γ GTP. (B) Changes in relative quantification of plasma in anti-fatigue and chronic stress biomarker with cortisol, GLU, and LDH. The data are the mean \pm standard error. The group comparisons ($n = 4$) were performed by one-way analysis of variance test. Tukey's $*P < .05$ compared with control. Abbreviations: ALP, alkaline phosphatase; ALT, alanine aminotransferase; AST, aspartate aminotransferase; BIL, bilirubin; γ -GTP, γ -glutamyl transpeptidase; GLU, glucose; LDH, lactate dehydrogenase.

We next investigated whether CMEAF could regulate cancer-related fatigue, which is influenced by the energy deficiency caused by loss of appetite following chemotherapy and the change in skeletal muscle metabolism and energy production.^{14,40-42} We measured fatigue-related biomarkers such as LDH, GLU, and cortisol in serum (Figure 4B). We found that the LDH level was higher in the control group, whereas there was a decrease in LDH levels in the treatment of CMEAF alone or in combination with sorafenib. In addition, GLU level in serum was significantly lower in the control group than in the treated groups, while CMEAF and sorafenib treated groups increased approximately 8.9% and 37.5%, respectively. Especially the level of GLU in combination treatment group showed dramatically increased up to 59.1%. In the level of cortisol as an indicator of mental cancer-related fatigue, CMEAF treatment greatly reduced the level of cortisol.

Effect of CMEAF to Liver Metabolic Changes

To further confirm that the improvement of hepatic function by CMEAF is tightly linked to the antifatigue effect, we conducted metabolomics analysis in liver tissues using $^1\text{H-NMR}$ spectroscopy. The assignment of the identified metabolites in the $^1\text{H-NMR}$ spectra is shown in Figure 5 and summarized in Table 1, which were identified with 5 sugars (glycocholate, methanol, GLU, glycerol, and

guanidinoacetate), 6 nucleic acids (uracil, uridine, ATP, xanthosine, adenine, and AMP), 10 organic acids (3-hydroxybutyrate, lactate, acetate, pyruvate, succinate, citrate, isocitrate, malonate, fumarate, and formate), 14 amino acids (isoleucine, leucine, valine, alanine, arginine, glutamate, glutamine, aspartate, asparagine, tyrosine, taurine, betaine, glycine, and phenylalanine), and 5 other molecules (trimethylamine (TMA), creatinine, creatine, choline, and niacinamide).

To compare the metabolic profiles of the 4 experimental groups, we performed the multivariate analyses of PCA and OPLS-DA. Although PCA score plots were generated and revealed no indication of discrimination among the 4 groups (Supplementary Figure S1), OPLS-DA multivariate analysis showed the unbiased clustering and supervised separation among the 4 groups (Figure 6A). The 4 groups were clearly separated with the OPLS-DA score plot model with an option of 2 predictive, 3 orthogonal X components, and 1 orthogonal Y component ($R^2X = 0.729$, $R^2Y = 0.648$, $Q^2 = 0.2$). In addition, we performed multivariate statistical analysis of the anti-fatigue indicators such as LDH and GLU and the 40 detected liver metabolites with OPLS regression (OPLSR) analysis, which indicated the relationship between the decomposition of X (metabolites from the xenograft mouse liver tissue NMR profiles) and the response matrix Y of the anti-fatigue indicators (LDH and GLU). OPLSR clearly

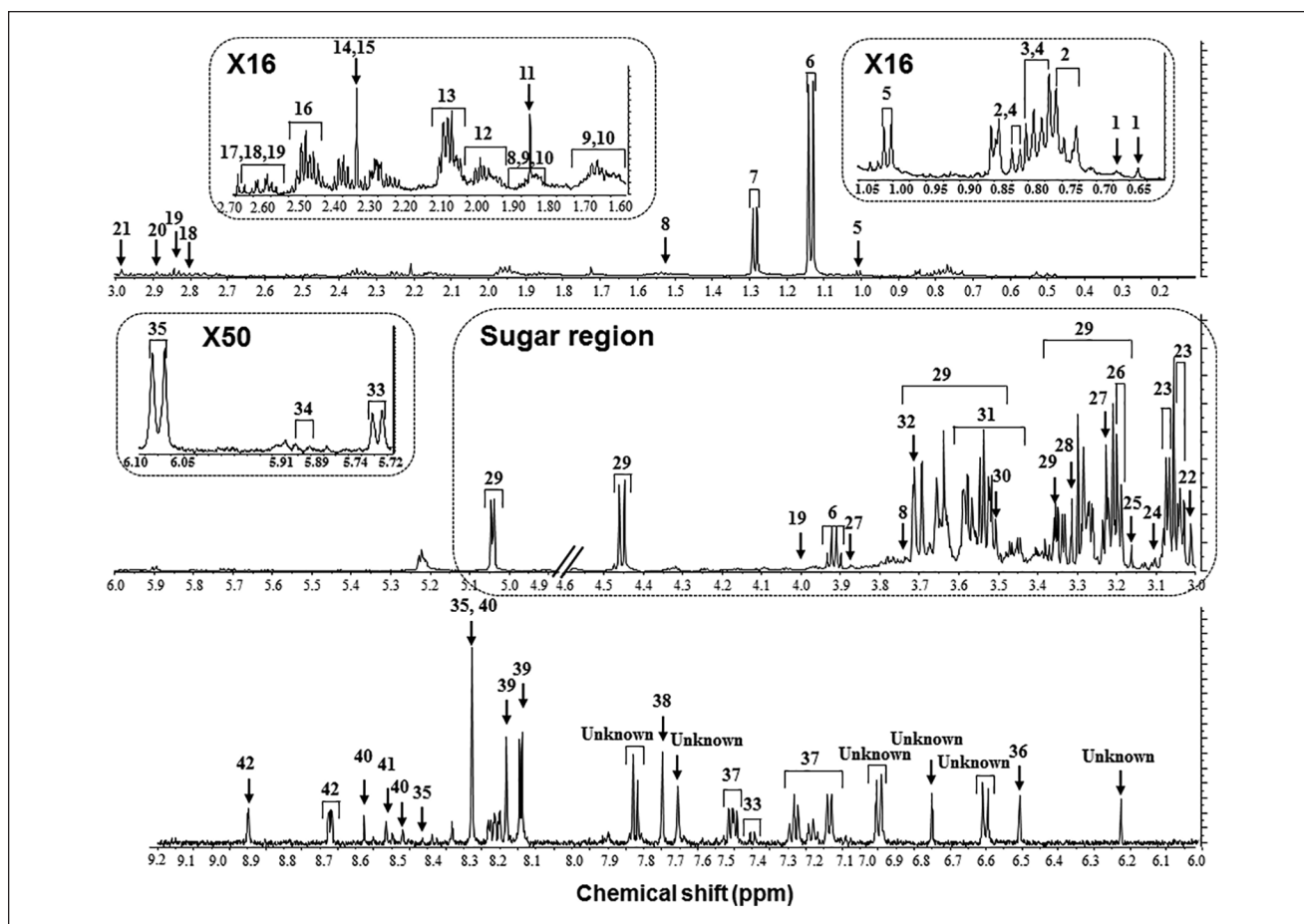


Figure 5. Regions of the 600 MHz ^1H -NMR spectra identification of liver tissue metabolites list described in Table I. The chemical shift of 40 liver tissue metabolites were indicated on the NMR spectrum. The top regions were multiplied by 16 times for better visualization and 1 to 20 metabolites were identified. In the middle region, 21 to 30 metabolites, such as sugar or sugar alcohol, were identified, and visualization was improved 50 times to identify 31 to 33 metabolites. In the bottom region, 34 to 40 metabolites, including unknown metabolites, were identified.

identified the NMR metabolite components that are relevant to anti-fatigue indicators. The correlation matrix exhibited a pair-wise correlation between X and Y variables, as determined with SIMCA +14 (Table 2). The correlation coefficient values of metabolites range from -1.0 to 1.0 . A total of 16 metabolites were considered significant when the absolute value of correlation coefficient is >0.4 . LDH was correlated with 6 metabolites, including lactate, pyruvate, isocitrate, TMA, ATP, and fumarate; and GLU was correlated with 10 metabolites, including isoleucine, leucine, valine, arginine, aspartate, asparagine, xanthosine, phenylalanine, adenine, and uracil (Table 2 and Figure 6B).

Discussion

Cordyceps militaris is a widely used traditional medicinal mushroom and has anticancer and anti-inflammatory

activities.^{43,44} In the present study, we confirmed in vivo anticancer and antifatigue effects of CMEAF. In a xenograft mouse model with Huh-7 HCC cell line, we evaluated in vivo efficacy of CMEAF alone or in combination with sorafenib for confirming the adjuvant effect. In addition, we analyzed biomarkers of hepatic function, including ALP, AST, BIL, and γGTP , and fatigue such as GLU and LDH in serum with biochemical analyze and investigated the metabolic changes in liver tissues using NMR analysis.

To select the most effective extract fraction in the inhibition of HCC proliferation, we prepared 5 different solvent extracts of *C. militaris* (Figure 1) and performed in vitro anticancer screening. CMEAF and CMBF markedly inhibited Huh-7 cell proliferation in a dose-dependent manner (Figure 2), and the IC_{50} values of CMEAF and CMBF were $14.4 \mu\text{g/mL}$ and $21.6 \mu\text{g/mL}$, respectively. Therefore, CMEAF showed the best inhibitory activity and was selected for further experiments.

Table 1. ¹H-NMR Chemical Shifts and Coupling Constants of Metabolites From the Liver Tissues.

No.	Metabolites	Chemical shift (δ) and coupling constants (J)
1	Glycocholate	δ 0.70 (s), δ 0.82 (s)
2	Isoleucine	δ 0.90 (t, $J = 6.5$ Hz), δ 1.02(d, $J = 6.9$ Hz)
3	Leucine	δ 0.94 (t, $J = 6.5$ Hz), δ 0.98 (m)
4	Valine	δ 0.98 (d, $J = 6.87$ Hz), δ 1.02 (d, $J = 6.0$ Hz)
5	3-Hydroxybutyrate	δ 1.18 (s)
6	Lactate	δ 1.3 (d, $J = 6.91$ Hz), δ 4.1 (dd, $J_1 = 6.71$ Hz, $J_2 = 13.06$ Hz)
7	Alanine	δ 1.46 (d, $J = 8.31$ Hz)
8	Citrulline	δ 1.54 (m), δ 1.86 (m), δ 3.74 (m)
9	Arginine	δ 1.66 (m), δ 1.70 (m), δ 1.90 (m)
10	Ornithine	δ 1.70 (m), δ 1.82 (m), δ 1.94 (m)
11	Acetate	δ 1.90 (s)
12	Glutamate	δ 2.02 (m)
13	Glutamine	δ 2.10 (m), δ 2.14 (m)
14	Pyruvate	δ 2.38 (s)
15	Succinate	δ 2.42 (s)
16	Citrate	δ 2.50 (d, $J = 15.92$ Hz), δ 2.66 (d, $J = 15.59$ Hz)
17	Isocitrate	δ 2.54 (m)
18	Aspartate	δ 2.62 (dd, $J_1 = 17.45$ Hz, $J_2 = 8.85$ Hz), δ 2.82 (dd, $J_1 = 17.45$ Hz, $J_2 = 3.72$ Hz)
19	Asparagine	δ 2.82 (m)
20	Trimethylamine	δ 2.89 (s)
21	Creatinine	δ 2.98 (s), δ 4.02 (s)
22	Creatine	δ 3.02 (s), δ 3.90 (s)
23	Tyrosine	δ 3.00 (dd, $J_1 = 8.0$ Hz, $J_2 = 8.0$ Hz), δ 3.08 (dd, $J_1 = 9.0$ Hz, $J_2 = 9.0$ Hz)
24	Malonate	δ 3.10 (s)
25	Choline	δ 3.18 (s)
26	Taurine	δ 3.22 (t, $J = 6.57$ Hz)
27	Betaine	δ 3.26 (s), δ 3.90 (s)
28	Methanol	δ 3.30 (s)
29	Glucose	δ 3.38 (t, $J = 8.9$ Hz), δ 3.46 (m), δ 3.50 (m), δ 3.86 (m), δ 4.62 (m), δ 5.20 (d, $J = 4.07$ Hz)
30	Glycine	δ 3.54 (s)
31	Glycerol	δ 3.54 (m), δ 3.60 (m)
32	Guanidoacetate	δ 3.78 (s)
33	Uracil	δ 5.78 (d, $J = 7.69$ Hz), δ 7.50 (d, $J = 7.68$ Hz)
34	Uridine	δ 5.90 (d, $J = 8.10$ Hz)
35	ATP	δ 6.06 (d, $J = 5.82$ Hz), δ 8.3 (s), δ 8.5 (s)
36	Fumarate	δ 6.5 (s)
37	Phenylalanine	δ 7.30 (m), δ 7.34 (m), δ 7.42 (m)
38	Xanthosine	δ 7.78 (s)
39	Adenosine	δ 8.16 (s), δ 8.18 (s)
40	AMP	δ 8.36 (s), δ 8.54 (s)
41	Formate	δ 8.43 (s)
42	Niacinamide	δ 8.70 (dd, $J_1 = 4.86$ Hz, $J_2 = 1.12$ Hz), δ 8.92 (s)

Next, we determined whether the combination of CMEAF with sorafenib shows adjuvant effects for anticancer and antifatigue compared with a single administration of CMEAF or sorafenib. In all treatment groups compared with control, tumor volume was significantly reduced (Figure 3) and the biochemical analyses showed the improvement of liver function, represented by increasing ALP and BIL levels and decreasing AST and γ GTP levels.

Additionally, the relief of cancer-related fatigue was explained by the increasing GLU level and decreasing LDH level (Figure 4).

According to multivariate statistical analysis from ¹H-NMR metabolic profiling, the metabolic changes in the liver tissues from the combination group were clearly separated from the control group (Figure 6A). The major metabolites that contributed to the separation along the

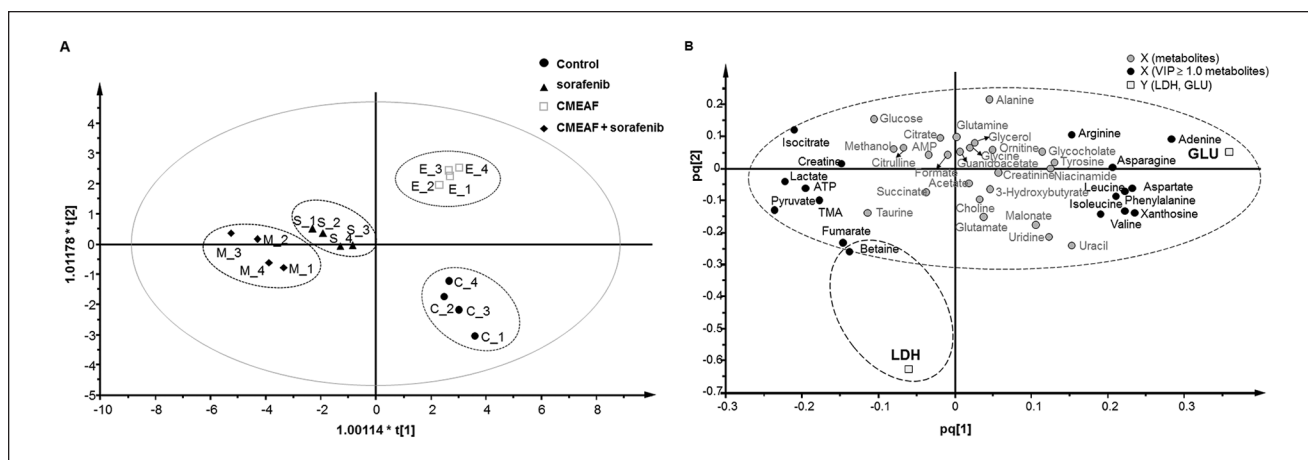


Figure 6. (A) OPLS-DA analysis of the liver tissue metabolites between control, sorafenib, *Cordyceps militaris* ethyl acetate extract fraction (CMEAF), and CMEAF with sorafenib. Score plot, green-colored circles, red-colored circles, blue-colored circles, and yellow-colored circles represented the control, sorafenib, CMEAF, and CMEAF with sorafenib-treated groups, respectively. (B) Correlation loading plot of the relationship between liver tissue metabolites and antifatigue biomarkers (lactate dehydrogenase [LDH] and glucose [GLU]). The loading score plot of the OPLS model, which is Y (LDH and GLU) variation correlated to X (metabolites) variation combined to one vector. The dark-colored circles represented variable importance in the projection (VIP) value over 1.0 and absolute $p(\text{corr})$ over 0.4. The gray-colored circles represented VIP value < 1.0 and absolute $p(\text{corr})$ under 0.4. The squared represented Y (LDH and GLU) variation.

partial least squares (PLS1) vector (positive: control, CMEAF) were as follows: creatine, betaine, GLU, fumarate, 3-hydroxybutyrate, AMP, TMA, pyruvate, lactate, taurine, isocitrate, and ATP. Also, aspartate, asparagine, malonate, tyrosine, arginine, xanthosine, valine, phenylalanine, creatinine, glycocholate, leucine, alanine, isoleucine, uridine, uracil, glycerol, glutamate, glycine, citrate, glutamine, niacinamide, guanidoacetate, succinate, methanol, choline, acetate, and formate were the major metabolites involved in the separation along the PLS1 vector (negative: sorafenib and CMEAF with sorafenib group). The metabolites located along the x -axis ($p[1]$) are important for separations between groups, while metabolites located along the y -axis ($p[2]$) contribute to within group variance (Supplementary Figure S2). To further investigate metabolites contributing the separation in OPLS-DA analysis, we calculated the score of VIP, which can be defined as a weighted sum of squares of the PLS weights. The variable importance in VIP score is an estimate of each variable (or a given predictor) in the projection used in a PLS model. A variable with a VIP score > 1.0 is important in the model, whereas VIP scores < 1.0 are considered less important and thus are generally excluded from the model. The 20 metabolites with VIP values over 1.0 were arginine, TMA, taurine, alanine, asparagine, leucine, ATP, betaine, lactate, isoleucine, phenylalanine, isocitrate, uridine, uracil, aspartate, valine, pyruvate, xanthosine, fumarate and adenine (Table 2). A total of 16 metabolites were

considered significant in the criteria of the absolute $p(\text{corr})$ value of > 0.4 (Supplementary Figure S3). These include ATP, isocitrate, lactate, pyruvate, fumarate, TMA, adenine, aspartate, asparagine, arginine, valine, isoleucine, leucine, phenylalanine, uracil, and xanthosine (Figure 6B). Among the 40 identified metabolites, isoleucine, leucine, valine, arginine, aspartate, asparagine, xanthosine, phenylalanine, adenine, and uracil were correlated with GLU.⁴⁵ Other metabolites lactate, pyruvate, isocitrate, TMA, ATP, and fumarate were correlated with LDH.⁴⁶ The GLU- and LDH-correlated metabolites were consistent with the molecules identified in the differentiating groups, as determined utilizing the VIP metric with a cutoff value > 1.0 and the loadings scaled as a correlation coefficient ($p[\text{corr}]$) value.

Conclusion

All together, these data demonstrate positive roles for CMEAF in both the inhibition of tumor growth and the alleviation of cancer-related fatigue. In addition, the change of liver metabolism by CMEAF is correlated with serum biomarkers of fatigue such as LDH and GLU. The combination of CMEAF with sorafenib showed the adjuvant effects in the suppression of tumor growth, the enhancement of hepatic functions, and the relief of cancer-related fatigue. Therefore, the combination therapy with sorafenib and CMEAF is a promising therapeutic strategy in liver cancer.

Table 2. Relative Intensity of Liver Tissue Metabolites and VIP Value With Correlation Matrix (LDH and GLU)^a.

Metabolites	Control	CMEAF	Sorafenib	CMEAF with sorafenib	VIP ^b	LDH ^c	GLU ^d
Sugars and alcohols							
Glycocholate	0.034 ± 0.0036*	0.035 ± 0.0051*	0.048 ± 0.0065*	0.040 ± 0.0041*	0.795	-0.113	0.302
Methanol	0.176 ± 0.0159*	0.154 ± 0.0177*	0.168 ± 0.0149*	0.170 ± 0.0092*	0.721	-0.086	-0.155
Glucose	10.965 ± 0.8248*	12.522 ± 0.7271*	10.470 ± 0.4965*	11.619 ± 1.5396*	0.977	-0.016	-0.294
Glycerol	1.237 ± 0.1374*	1.413 ± 0.0745*	1.311 ± 0.2136*	1.670 ± 0.2718*	0.798	-0.119	0.053
Guanidoacetate	0.751 ± 0.1218*	0.789 ± 0.0506*	0.726 ± 0.0912*	0.865 ± 0.1338*	0.796	-0.051	0.025
Nucleic acids							
Uracil ¹	0.023 ± 0.0028*	0.022 ± 0.0031*	0.028 ± 0.0024*	0.027 ± 0.0023*	1.273	0.303	0.388
Uridine ¹	0.037 ± 0.0025*	0.035 ± 0.0016*	0.041 ± 0.0034*	0.044 ± 0.0062*	1.210	0.244	0.323
AMP	0.036 ± 0.0023*	0.038 ± 0.0020*	0.037 ± 0.0020*	0.033 ± 0.0009*	0.760	-0.018	-0.182
ATP ^{1,3}	0.153 ± 0.0018*	0.160 ± 0.0055*	0.132 ± 0.0145*	0.111 ± 0.0082*	1.107	0.148	-0.566
Adenine ^{1,3}	0.052 ± 0.0036*	0.062 ± 0.0051*	0.080 ± 0.0059*	0.090 ± 0.0044*	1.397	-0.269	0.782
Xanthosine ^{1,3}	0.029 ± 0.0023*	0.030 ± 0.0035*	0.035 ± 0.0048*	0.040 ± 0.0018*	1.306	0.070	0.601
Organic acids							
3-Hydroxybutyrate	0.083 ± 0.0058*	0.103 ± 0.0064*	0.093 ± 0.0044*	0.089 ± 0.0061*	0.445	0.108	0.032
Lactate ^{1,3}	4.529 ± 0.1953*	4.939 ± 0.1955*	4.207 ± 0.2761*	3.975 ± 0.1814*	1.119	0.205	-0.613
Acetate	0.101 ± 0.0090*	0.121 ± 0.0044*	0.125 ± 0.0167*	0.105 ± 0.0067*	0.398	-0.061	-0.039
Pyruvate ^{1,3}	0.184 ± 0.0055*	0.168 ± 0.0181*	0.145 ± 0.0223*	0.130 ± 0.0083*	1.226	0.141	-0.654
Succinate	0.164 ± 0.0050*	0.155 ± 0.0140*	0.159 ± 0.0063*	0.162 ± 0.0102*	0.608	0.137	-0.099
Citrate	0.280 ± 0.0136*	0.287 ± 0.0196*	0.298 ± 0.0167*	0.289 ± 0.0070*	0.812	-0.109	-0.024
Citrulline	1.727 ± 0.1546*	1.923 ± 0.1383*	1.726 ± 0.1475*	1.915 ± 0.2219*	0.798	0.001	-0.105
Isocitrate ^{1,3}	0.210 ± 0.0172*	0.220 ± 0.0191*	0.190 ± 0.0174*	0.148 ± 0.0052*	1.180	-0.100	-0.534
Malonate	0.084 ± 0.0044*	0.077 ± 0.0038*	0.117 ± 0.0159*	0.125 ± 0.0141*	1.050	0.282	0.309
Fumarate ^{1,3}	0.017 ± 0.0008*	0.017 ± 0.0014*	0.016 ± 0.0023*	0.015 ± 0.0023*	1.319	0.373	-0.441
Formate	0.013 ± 0.0007*	0.012 ± 0.0006*	0.013 ± 0.0013*	0.014 ± 0.0025*	0.707	0.109	0.030
Amino acids							
Isoleucine ^{1,3}	0.147 ± 0.0096*	0.188 ± 0.0246*	0.194 ± 0.0227*	0.207 ± 0.0167*	1.168	0.165	0.493
Leucine ^{1,3}	0.301 ± 0.0151*	0.449 ± 0.0884*	0.458 ± 0.0534*	0.498 ± 0.0117*	1.123	0.011	0.589
Valine ^{1,3}	0.238 ± 0.0134*	0.301 ± 0.0384*	0.353 ± 0.0489*	0.379 ± 0.0168*	1.261	0.094	0.598
Alanine ¹	0.835 ± 0.0531*	0.933 ± 0.0685*	0.887 ± 0.0596*	1.005 ± 0.0265*	1.052	-0.292	0.177
Arginine ^{1,3}	0.195 ± 0.0154*	0.223 ± 0.0057*	0.252 ± 0.0281*	0.262 ± 0.0091*	1.003	-0.220	0.425
Glutamate	0.083 ± 0.0055*	0.071 ± 0.0043*	0.081 ± 0.0105*	0.087 ± 0.0053*	0.869	0.190	0.151
Glutamine	0.468 ± 0.0153*	0.523 ± 0.0339*	0.531 ± 0.0452*	0.490 ± 0.0141*	0.727	-0.186	0.052
Aspartate ^{1,3}	0.089 ± 0.0036*	0.078 ± 0.0057*	0.117 ± 0.0120*	0.148 ± 0.0050*	1.216	0.047	0.673
Asparagine ^{1,3}	0.059 ± 0.0057*	0.040 ± 0.0053*	0.068 ± 0.0075*	0.090 ± 0.0037*	1.067	-0.060	0.616
Tyrosine ³	0.161 ± 0.0078*	0.153 ± 0.0182*	0.214 ± 0.0153*	0.209 ± 0.0201*	0.904	-0.114	-0.418
Taurine ¹	3.306 ± 0.0765*	2.953 ± 0.1195*	2.923 ± 0.1993*	2.664 ± 0.0745*	1.014	0.227	-0.321
Phenylalanine ^{1,3}	0.079 ± 0.0071*	0.085 ± 0.0065*	0.113 ± 0.0188*	0.123 ± 0.0037*	1.193	0.011	0.584
Betaine ^{1,2,3}	3.206 ± 0.1853*	3.168 ± 0.2333*	3.047 ± 0.1994*	3.210 ± 0.2834*	1.328	0.560	-0.437
Glycine	1.017 ± 0.0865*	1.141 ± 0.0473*	1.055 ± 0.1444*	1.265 ± 0.1280*	0.832	-0.083	0.053
Ornithine	1.019 ± 0.1237*	1.060 ± 0.0556*	1.044 ± 0.1072*	1.230 ± 0.1416*	0.842	-0.090	0.148
Others							
Trimethylamine ^{1,3}	0.081 ± 0.0052*	0.071 ± 0.0105*	0.070 ± 0.0144*	0.051 ± 0.0025*	1.042	0.202	-0.442
Creatinine	0.154 ± 0.0069*	0.145 ± 0.0183*	0.202 ± 0.0244*	0.213 ± 0.0273*	0.918	-0.102	0.336
Creatine ³	1.445 ± 0.1139*	1.610 ± 0.1102*	1.415 ± 0.0722*	1.552 ± 0.1793*	0.928	0.172	-0.418
Choline	0.360 ± 0.0119*	0.299 ± 0.0443*	0.340 ± 0.0447*	0.355 ± 0.0127*	0.723	0.068	0.128
Niacinamide	0.083 ± 0.0027*	0.085 ± 0.0018*	0.086 ± 0.0077*	0.086 ± 0.0034*	0.769	-0.061	0.150

Abbreviations: VIP, variable importance in the projection; LDH, lactate dehydrogenase; GLU, glucose; CMEAF, *Cordyceps militaris* ethyl acetate extract fraction; TSP, sodium 3-(trimethylsilyl)-propionic-2,2,3,3-d₄ acid sodium salt.

^aThe relative intensity was calculated by dividing each compound by the TSP of internal standard, its relative intensity shown as the mean ± standard error of the mean values for each biochemical compound was obtained with biological quadruple (n = 4). The significant differences in metabolite levels were evaluated by one-way analysis of variance using the SPSS statistics software (version 22.0, SPSS Inc) followed by the Duncan's significant-difference test. And different superscript numerals indicate significant differences (*p < 0.05).

^bVIP value more than 0.9.

^cLDH-correlated metabolites.

^dGLU-correlated metabolites.

Declaration of Conflicting Interests

The author(s) declared no potential conflicts of interest with respect to the research, authorship, and/or publication of this article.

Funding

The author(s) disclosed receipt of the following financial support for the research, authorship, and/or publication of this article: This research was supported by Bio-industry Technology Development Program (316025-05) of IPET (Korea Institute of Planning and Evaluation for Technology in Food, Agriculture, Forestry, and Fisheries), the National Research Foundation (NRF) grant funded by the Korea government (MSIT; No. 2019R1A2C2005157), and a research fund from Catholic Kwandong University (CKURF 201805590001).

ORCID iD

Enhyun Choi  <https://orcid.org/0000-0002-8464-7156>

Supplemental Material

Supplemental material for this article is available online.

References

- Farazi PA, DePinho RA. Hepatocellular carcinoma pathogenesis: from genes to environment. *Nat Rev Cancer*. 2006;6:674-687.
- Tang WY, Chau SP, Tsang WP, Kong SK, Kwok TT. The role of Raf-1 in radiation resistance of human hepatocellular carcinoma Hep G2 cells. *Oncol Rep*. 2004;12:1349-1354.
- Ibrahim N, Yu Y, Walsh WR, Yang JL. Molecular targeted therapies for cancer: sorafenib mono-therapy and its combination with other therapies. *Oncol Rep*. 2012;27:1303-1311.
- Brose MS, Frenette CT, Keefe SM, Stein SM. Management of sorafenib-related adverse events: a clinician's perspective. *Semin Oncol*. 2014;41(suppl 2):S1-S16.
- Sajithlal GB, Hamed HA, Cruickshanks N, et al. Sorafenib/regorafenib and phosphatidylinositol 3 kinase/thymoma viral proto-oncogene inhibition interact to kill tumor cells. *Mol Pharmacol*. 2013;84:562-571.
- Lachenmayer A, Toffanin S, Cabellos L, et al. Combination therapy for hepatocellular carcinoma: additive preclinical efficacy of the HDAC inhibitor panobinostat with sorafenib. *J Hepatol*. 2012;56:1343-1350.
- Cervello M, Bachvarov D, Lampiasi N, et al. Novel combination of sorafenib and celecoxib provides synergistic anti-proliferative and pro-apoptotic effects in human liver cancer cells. *PLoS One*. 2013;8:e65569.
- Lin Y, Lin L, Jin Y, Wang D, Tan Y, Zheng C. Combination of matrine and sorafenib decreases the aggressive phenotypes of hepatocellular carcinoma cells. *Chemotherapy*. 2014;60:112-118.
- Rong LW, Wang RX, Zheng XL, et al. Combination of wogonin and sorafenib effectively kills human hepatocellular carcinoma cells through apoptosis potentiation and autophagy inhibition. *Oncol Lett*. 2017;13:5028-5034.
- Flaherty KT, Lee SJ, Zhao F, et al. Phase III trial of carboplatin and paclitaxel with or without sorafenib in metastatic melanoma. *J Clin Oncol*. 2013;31:373-379.
- Ray M, Rogers LQ, Trammell RA, Toth LA. Fatigue and sleep during cancer and chemotherapy: translational rodent models. *Comp Med*. 2008;58:234-245.
- Berger AM, Farr LA, Kuhn BR, Fischer P, Agrawal S. Values of sleep/wake, activity/rest, circadian rhythms, and fatigue prior to adjuvant breast cancer chemotherapy. *J Pain Symptom Manage*. 2007;33:398-409.
- Kimel M, Leidy NK, Mannix S, Dixon J. Does epoetin alfa improve health-related quality of life in chronically ill patients with anemia? Summary of trials of cancer, HIV/AIDS, and chronic kidney disease. *Value Health*. 2008;11:57-75.
- Mock V, Atkinson A, Barsevick A, et al. NCCN practice guidelines for cancer-related fatigue. *Oncology (Williston Park)*. 2000;14:151-161.
- Kume S, Yamato M, Tamura Y, et al. Potential biomarkers of fatigue identified by plasma metabolome analysis in rats. *PLoS One*. 2015;10:e0120106.
- Wang J, Li S, Fan Y, et al. Anti-fatigue activity of the water-soluble polysaccharides isolated from Panax ginseng C. A. Meyer. *J Ethnopharmacol*. 2010;130:421-423.
- Liu R, Wu L, Du Q, et al. Small molecule oligopeptides isolated from walnut (*Juglans regia* L.) and their anti-fatigue effects in mice. *Molecules*. 2018;24:45.
- Jung K, Kim IH, Han D. Effect of medicinal plant extracts on forced swimming capacity in mice. *J Ethnopharmacol*. 2004;93:75-81.
- Kim H, Park S, Han DS, Park T. Octacosanol supplementation increases running endurance time and improves biochemical parameters after exhaustion in trained rats. *J Med Food*. 2003;6:345-351.
- Shang H, Cao S, Wang J, Zheng H, Putheti R. Glabridin from Chinese herb licorice inhibits fatigue in mice. *Afr J Tradit Complement Altern Med*. 2009;7:17-23.
- Li M, Donglian C, Huaixing L, Bende T, Lihua S, Ying W. Anti-fatigue effects of salidroside in mice. *J Med Coll PLA*. 2008;23:88-93.
- Li ZY, He P, Sun HF, Qin XM, Du GH. ¹H NMR based metabolomic study of the antifatigue effect of Astragali Radix. *Mol Biosyst*. 2014;10:3022-3030.
- Sung GH, Hywel-Jones NL, Sung JM, Luangsa-Ard JJ, Shrestha B, Spatafora JW. Phylogenetic classification of *Cordyceps* and the clavicipitaceous fungi. *Stud Mycol*. 2007;57:5-59.
- Wong JH, Sze SCW, Ng TB, et al. Apoptosis and anti-cancer drug discovery: the power of medicinal fungi and plants. *Curr Med Chem*. 2018;25:5613-5630.
- Das SK, Masuda M, Sakurai A, Sakakibara M. Medicinal uses of the mushroom *Cordyceps militaris*: current state and prospects. *Fitoterapia*. 2010;81:961-968.
- Shrestha B, Zhang W, Zhang Y, Liu X. The medicinal fungus *Cordyceps militaris*: research and development. *Mycol Prog*. 2012;11:599-614.
- Tuli HS, Sandhu SS, Sharma AK. Pharmacological and therapeutic potential of *Cordyceps* with special reference to Cordycepin. *3 Biotech*. 2014;4:1-12.

28. Song J, Wang Y, Teng M, et al. Studies on the antifatigue activities of *Cordyceps militaris* fruit body extract in mouse model. *Evid Based Complement Alternat Med*. 2015;2015:174616.
29. Song J, Wang Y, Teng M, et al. *Cordyceps militaris* induces tumor cell death via the caspase-dependent mitochondrial pathway in HepG2 and MCF7 cells. *Mol Med Rep*. 2016;13:5132-5140.
30. Kim DJ, Kang YH, Kim KK, Kim TW, Park JB, Choe M. Increased glucose metabolism and alpha-glucosidase inhibition in *Cordyceps militaris* water extract-treated HepG2 cells. *Nutr Res Pract*. 2017;11:180-189.
31. Zhong L, Zhao L, Yang F, Yang W, Sun Y, Hu Q. Evaluation of anti-fatigue property of the extruded product of cereal grains mixed with *Cordyceps militaris* on mice. *J Int Soc Sports Nutr*. 2017;14:15.
32. Dong Y, Hu S, Liu C, et al. Purification of polysaccharides from *Cordyceps militaris* and their antihypoxic effect. *Mol Med Rep*. 2015;11:1312-1317.
33. Liu X, Locasale JW. Metabolomics: a primer. *Trends Biochem Sci*. 2017;42:274-284.
34. Ji Y, Cao Y, Song Y. Green synthesis of gold nanoparticles using a *Cordyceps militaris* extract and their antiproliferative effect in liver cancer cells (HepG2). *Artif Cells Nanomed Biotechnol*. 2019;47:2737-2745.
35. Zhou Q, Zhang Z, Song L, et al. *Cordyceps militaris* fraction inhibits the invasion and metastasis of lung cancer cells through the protein kinase B/glycogen synthase kinase 3beta/beta-catenin signaling pathway. *Oncol Lett*. 2018;16:6930-6939.
36. Choi HN, Jang YH, Kim MJ, et al. *Cordyceps militaris* alleviates non-alcoholic fatty liver disease in ob/ob mice. *Nutr Res Pract*. 2014;8:172-176.
37. Pratt DS, Kaplan MM. Evaluation of abnormal liver-enzyme results in asymptomatic patients. *N Engl J Med*. 2000;342:1266-1271.
38. Limdi JK, Hyde GM. Evaluation of abnormal liver function tests. *Postgrad Med J*. 2003;79:307-312.
39. Cynober L, Le Boucher J, Vasson MP. Arginine metabolism in mammals. *J Nutr Biochem*. 1995;6:402-413.
40. Hur H. Chemical ingredients of *Cordyceps militaris*. *Mycobiology*. 2008;36:233-235.
41. Xu S, Tian Y, Hu Y, et al. Tumor growth affects the metabolomic phenotypes of multiple mouse non-involved organs in an A₅₄₉ lung cancer xenograft model. *Sci Rep*. 2016;6:28057.
42. Sales RP, Miné CEC, Franco AD, et al. Effects of the acute arginine aspartate supplement on the muscular fatigue in trained volunteers. *Rev Bras Med Esporte*. 2005;11:347-351.
43. Park JG, Son YJ, Lee TH, et al. Anticancer efficacy of *Cordyceps militaris* ethanol extract in a xenografted leukemia model. *Evid Based Complement Alternat Med*. 2017;2017:8474703.
44. Smiderle FR, Baggio CH, Borato DG, et al. Anti-inflammatory properties of the medicinal mushroom *Cordyceps militaris* might be related to its linear (1-3)-β-D-glucan. *PLoS One*. 2014;9:e110266.
45. Ho JE, Larson MG, Vasani RS, et al. Metabolite profiles during oral glucose challenge. *Diabetes*. 2013;62:2689-2698.
46. Valvona CJ, Fillmore HL, Nunn PB, Pilkington GJ. The regulation and function of lactate dehydrogenase A: therapeutic potential in brain tumor. *Brain Pathol*. 2016;26:3-17.